

6 Evolutionary Lock-In and the Origin of Modularity in RNA Structure

Lauren Ancel Meyers and Walter Fontana

Modularity is a hallmark of biological organization and an important source of evolutionary novelty (Bonner, 1988; Wagner and Altenberg, 1996; Hartwell et al., 1999). Yet, the origin of modules remains a problem for evolutionary biology, even in the case of the most basic protein or RNA domains (Westhof et al., 1996). Biological modularity has been defined on many levels, including genetic, morphological, and developmental. The task of creating a general theory for the origins, ubiquity, and function of modularity requires the synthesis of these perspectives.

The first step in understanding the causes and consequences of modularity is to define modularity. The second step is to formulate methods of detecting it. The third is to build models and design experiments to study its origins and evolutionary implications.

In this chapter we offer a rigorous definition of modularity in RNA. It is the partitioning of molecules into subunits that are simultaneously independent with respect to their thermodynamic environment, genetic context, and folding kinetics. On the variational level, the module consists of a stretch (or stretches) of contiguous ribonucleotides held together by a covalent backbone. On the functional level, the relevant interactions include the covalent bonds of adjacent ribonucleotides and hydrogen bonds between nonadjacent bases. These elements of secondary structure provide the scaffold for tertiary structure, which underlies the functionality of the molecule.

We furthermore offer a practical tool for identification of modules in this semi-empirical framework. The melting profile of a molecule is the set of minimum free energy shapes attained as the temperature increases from 0° to 100° C. Modules are exactly those subunits that dissolve discretely without perturbing the remaining structure as temperature increases. A modular molecule is one made up entirely of such subunits.

Finally, we present a theory about the origins of modularity. Modularity may facilitate the evolution of more complex organisms through the combination of modules. If we try to explain the origins of modularity in terms of this evolutionary benefit, we run into a chicken-and-egg paradox. Modularity cannot produce a more sophisticated syntax of variation until it already exists.

Here we offer a more agnostic explanation for the evolution of modularity. Using a model of RNA folding, we show that modularity arises as a by-product when natural selection acts to reduce the plasticity of molecules by stabilizing their shapes. This is mediated by a statistical property of the RNA folding map: the more thermodynamically well-defined a shape, the more localized and less disruptive the

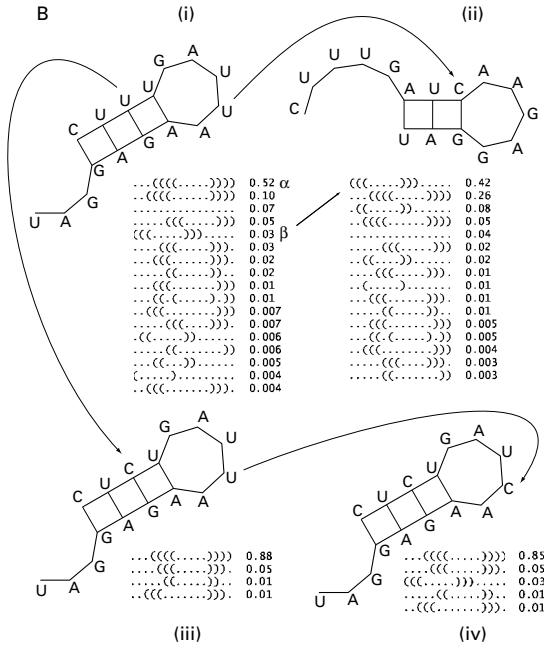
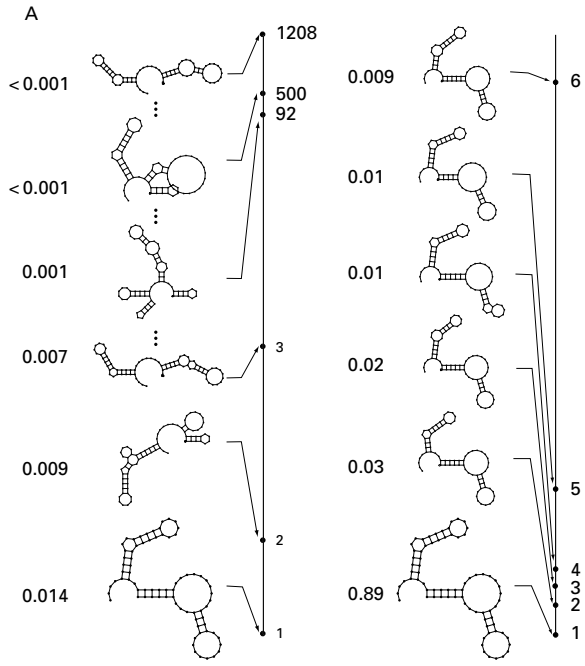
effects of point mutations. We report two consequences of this relationship. First, under selection for thermodynamic stability, evolution grinds to a halt because of insufficient phenotypic variation. Second, the shapes trapped in this exploration catastrophe are highly modular. They consist of structural units that have become thermophysically, kinetically, and genetically independent.

Plasticity in RNA Secondary Structure

Under natural conditions, RNA molecules do not freeze in their minimum free-energy shape (henceforth ground state), but exhibit a form of structural plasticity. Thermal fluctuations (corresponding to environmental noise) cause molecules to equilibrate among alternative low-energy shapes. We model the genotype–phenotype map from an RNA sequence to its repertoire of alternative secondary structures (henceforth shapes), using an extension (Wuchty et al., 1999) of standard algorithms (Nussinov and Jacobson, 1980; Waterman, 1978; Zuker and Stiegler, 1981) which assist in the prediction of RNA secondary structure. For a given sequence, we compute all possible shapes having free energy within 3 kcal/mol of the ground state (at 37°C). We call this set of shapes the “plastic repertoire” of an RNA sequence (see figure 6.1A for an illustration). The partition function (McCaskill, 1990) of a sequence is $Z = \sum_{\alpha} \exp(-\Delta G_{\alpha}/kT)$, where ΔG_{α} is the free

Figure 6.1

Loss of plasticity and plastogenetic congruence. (A) On the right: all six shapes in the plastic repertoire of the most frequent sequence after 10^7 replications in the plastic simulation depicted in Figure 6.2A. The few shapes in the plastic repertoire of the evolved sequence are structurally similar to each other and the ground state. On the left: a subset of the 1208 shapes in the plastic repertoire of a randomly chosen sequence with the same ground state. Dots stand for many shapes not displayed. The number to the left of a shape is its equilibrium probability. The vertical lines on the right measure 3 kcal/mol, and each shape points to a height proportional to its energetic distance from the minimum free energy. (B) The graph illustrates the mechanisms underlying plastogenetic congruence in a small sequence. Aside from a graphical depiction of shapes, we also use a string representation in which a dot stands for an unpaired position, and a pair of matching parentheses indicates positions that pair with one another. A highly plastic sequence (i) is shown in its ground state shape α together with a list of all shapes in its plastic repertoire (numbers indicate equilibrium probabilities). Single-point mutations readily tip the energy balance in favor of another shape. For example, a point mutation from U to C in the loop of (i) makes its suboptimal shape β the new ground state in (ii). Generally, single-point mutations tip a highly plastic sequence in favor of shapes already present in its plastic repertoire. Single-point mutations can also act to reinforce the ground state. For example, a mutation from U to C (iii) generates a better stacking pair in the helix of α , and dramatically reduces the plasticity. As a consequence, the mutation that altered the ground state shape previously, (i) \rightarrow (ii), no longer has a phenotypic effect, (iii) \rightarrow (iv). Thermodynamic stabilization dramatically decreases variability—access to new structures through mutation.



energy of shape α and the sum runs over all possible shapes into which the sequence can fold. For any shape σ in the plastic repertoire of the sequence, the Boltzmann probability of σ , $p_\sigma = \exp(-\Delta G_\sigma/kT)/Z$, measures the relative stability of σ with respect to the entire repertoire. Assuming equilibration, p_σ is the amount of time the RNA molecule resides in shape σ . The ground state is the most probable shape for a molecule.

The Loss of Plasticity and Evolvability

Equipped with this computational model of RNA, we simulate an experimental protocol that evolves molecules to optimally bind a ligand (Ellington, 1994). We select sequences according to their similarity to a prespecified target shape (Fontana and Schuster, 1998). In nature, the plasticity of an RNA sequence will presumably influence the overall binding constant of the molecule. At equilibrium, a fraction p_σ of a large number of identical sequences assumes shape σ and binds to ligand with the corresponding constant. In our model we proceed similarly by calculating for each shape σ in the plastic repertoire a selective value $f(\sigma)$ based on how well σ matches the target shape. The overall selective value, or fitness, r of the sequence is the average of the selective values of the shapes in its plastic repertoire, each weighted by its occupancy time, $r = \sum_\alpha f(\sigma)p_\sigma$. Point mutations provide the sole source of genetic variation in our simulations. This completes the model.

In order to identify the evolutionary implications of plasticity, we compare simulations of plastic RNA populations with simulations of nonplastic control populations. Sequences in the control populations rigidly fold into the ground state only. Consequently, selection does not consider other low-energy shapes or the thermodynamic stability of the ground state.

High plasticity, that is, a large and diverse plastic repertoire, can be advantageous since multiple shapes, rather than just the ground state, contribute to the fitness of a sequence. In particular, a plastic sequence can partially offset a bad ground state with a good alternative shape in its repertoire. Yet plasticity is ultimately costly. The more shapes a molecule has in its plastic repertoire, the less time it spends in any one of them, including advantageous shapes. The evolutionary scenario under consideration—selection toward a constant target shape—must eventually favor the reduction of plasticity. The dynamics resemble a Simpson–Baldwin Effect, in which organisms gain and then lose plasticity as they adapt to a novel environment (Ancel, 1999; Baldwin, 1896). Figure 6.1A illustrates the plastic repertoire of a typical sequence present at the end of a plastic simulation (right). A comparison with a randomly chosen sequence folding into the same ground state (left) reveals the

staggering reduction in plasticity. The number of shapes in the plastic repertoire decreases 200-fold, the fraction of time spent in the ground state increases from 1.4% to 89%, and structural diversity within the 3kcal band is nearly eliminated. Sequences found at the end of such simulations have well-defined ground states that are extremely resilient to thermal fluctuations.

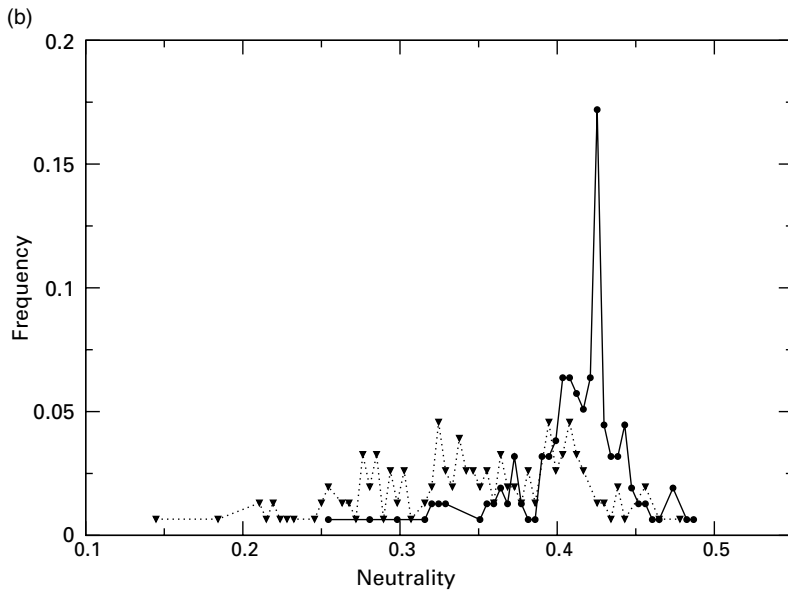
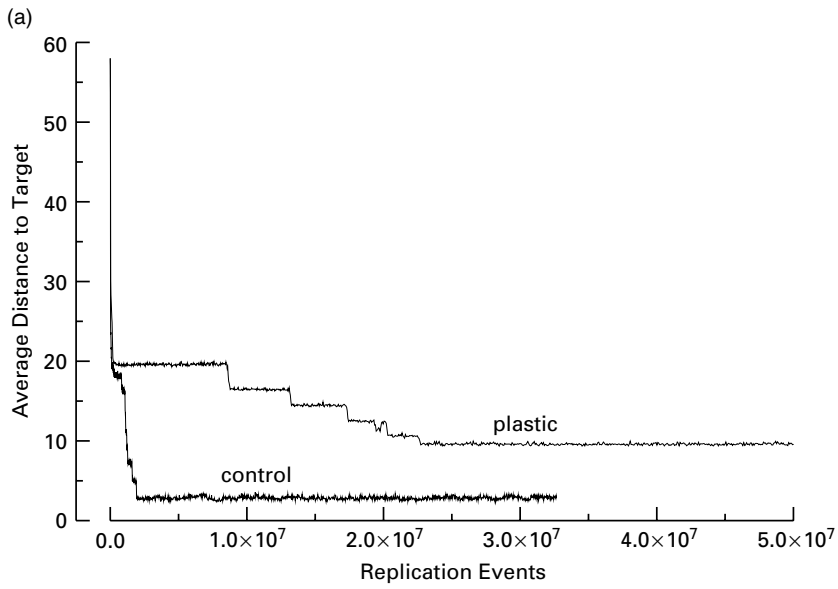
This reduction in plasticity produces a remarkable effect evident in the evolutionary trajectories of typical plastic and control populations (figure 6.2A). Surprisingly, the population of plastic sequences evolves more slowly than the non-plastic control population, and quickly reaches an evolutionary dead end. Both evolve in a stepwise fashion with periods of phenotypic stasis punctuated by change toward the target shape (Ancel and Fontana, 2000; Fontana and Schuster, 1998).

Plastogenetic Congruence

The loss of evolvability stems from a statistical correlation between the thermodynamic plasticity of an RNA molecule and the mutability of its ground state structure through point mutations (Simpson, 1953). In particular, thermodynamic robustness (or lack of plasticity) is positively correlated to mutational robustness. Mutations which stabilize the ground state of a molecule also serve to buffer the molecule against structural changes due to mutations. Figure 6.1B illustrates the mechanism underlying this correlation. A highly plastic molecule wiggles among multiple alternative shapes that are energetically close to one another. A point mutation can easily tip the energy landscape of the molecule in favor of an alternative shape (without destroying sequence compatibility with the original ground state). This occurs in the transition from (i) to (ii), where the alternative shape β becomes the new ground state. At the same time, a plastic molecule also offers opportunities to stabilize a ground state, as in the transition from (i) to (iii). Note, however, that along with this reinforcement comes the immunity of the ground state to a point mutation which affected it in the previous sequence context, as in (iii) to (iv) versus (i) to (ii).

This capability of genes (or, in this case, ribonucleotides) to buffer other genes against the effects of mutations is known as epistasis. More generally, epistasis is the nonindependence of loci. When the fitness consequence of a mutation at one site depends on the nucleotides present at other sites, then there is epistasis between the sites. In RNA we observe the evolution of epistatic buffering, where critical base pairs render the minimum free-energy structure robust to most point mutations.

In summary, the plastic repertoire of an RNA molecule indicates how much and in which ways its ground state can be altered by mutation. We call this statistical



alignment between the thermodynamic sensitivity of the ground state and its genetic mutability *plastogenetic congruence*. We emphasize that this is not an assumption of our model, but a hitherto unknown statistical property of RNA folding algorithms that were developed independently of our evolutionary study. A similar correlation between the thermodynamic stability of the native conformation and its mutational robustness has been found in models of protein folding (Bornberg-Bauer and Chan, 1999; Vendruscolo et al., 1997; Bussemaker et al., 1997).

What are the consequences of plastogenetic congruence for our evolutionary model? Natural selection produces sequences with low plasticity (figure 6.1A). Low plasticity sequences are, by virtue of plastogenetic congruence, highly buffered against the effects of mutation. A large fraction of all possible single-point mutations on such sequences will preserve the ground state (figure 6.2B). Furthermore, the low-plasticity sequences not only reside mostly in their ground state, but spend the rest of their time in shapes that are structurally akin to it (figure 6.1A). Again, by plastogenetic congruence, the rare mutations that alter the ground state are likely to cause only slight structural changes. Thus, the phenotypic variability of the population, that is, the potential variation accessible through mutation, is dramatically curtailed. Plastogenetic congruence has steered the population into an evolutionary dead end which we call *neutral confinement*. This does not occur in the control populations (figure 6.2A).



Figure 6.2

Evolutionary dynamics and neutral confinement. (A) A simulated population of RNA sequences undergoes mutation, replication, and selection in a chemical flow reactor constrained to fluctuate around 1000 individuals. This process models a stochastic continuous-time chemical reaction system (Fontana and Schuster, 1998; Huynen et al., 1996). We graph the average population distance from the target shape with respect to replication events rather than external time. The selective value $f(\sigma)$ of a shape σ is defined in terms of the Hamming distance $d(\sigma, \tau)$ between the string representations (see caption for figure 6.1B)

of σ and the target shape τ : $f(\sigma) = \frac{1}{0.01 + d(\sigma, \tau)/n}$ where n is the sequence length (here $n = 76$). The

fitness (or replication constant) of a plastic sequence is given as $r = \sum_{\sigma_i} f(\sigma_i) \frac{\exp(-\Delta G_{\sigma_i}/kT)}{z}$, where

the sum runs over all shapes σ_i with free energies ΔG_{σ_i} within 3 kcal/mol from the minimum free energy. The control population comprises sequences that are mapped simply to their minimum free-energy shapes σ_0 , and hence have fitness $r = f(\sigma_0)$. Replication accuracy per position is 0.999. (B) For each sequence species present in a given population, we compute its neutrality, that is, the fraction of single-point mutants that preserve the ground state. The graph compares the distributions of neutralities for the plastic population (solid line) and the nonplastic control (dotted line) after 10^7 replications.

Origins of Modularity

Low plasticity is achieved through increasing the thermodynamic independence of any one structural component from the remaining structure. At the same time, the effects (if any) of mutations become increasingly limited to local shape features. Wagner and Altenberg (1996) argued that modularity evolves in organisms by such a decrease of pleiotropy. This process underlies the extreme modularity of ground states that we observe at neutral confinement. We distinguish here between modules defined in purely morphological (syntactical) terms and modules defined on the basis of thermophysical, kinetic, and genetic autonomy. The former is a trivial notion in RNA, since it is implicit in the very definition of a secondary structure as a combination of loops and helices. We address the latter. (In the case of RNA secondary structures, these two notions are conveniently consistent with each other: the thermodynamic stabilization of the ground state as a whole can easily proceed through the stabilization of its component helices and loops.)

From a thermophysical perspective, low-plasticity shapes are composed of structural components that remain intact over large temperature regimes and that melt in distinct phase transitions as discrete units (figure 6.3A). In particular, the melting of one unit does not disturb the other units (figure 6.3B). This is in sharp contrast to the melting behavior of high-plasticity sequences with the same ground state (figures 6.3A and 6.3C). From a kinetic perspective, these same units fold independently, as suggested by a single folding funnel which dominates the energy landscape of a low-plasticity sequence (figure 6.3D). A conformational energy landscape so organized prevents the occurrence of energetically trapped intermediates by guiding the folding events reliably and quickly toward the ground state. Again, this is in sharp contrast to the high-plasticity sequence, whose energy landscape provides no guidance to the folding process (figure 6.3E).

Genetic autonomy is seen when sequence segments underlying these structural units are transposed from their original context into random contexts. Low-plasticity segments maintain their original shape with a much higher likelihood than the fragments of random sequences with the same shape. For example, the sequence segments underlying the shape features labeled A and B in figure 6.3B maintain their original shape with probabilities 0.83 and 0.94, respectively, when flanked by random segments of half their size. These are much larger than the probabilities 0.017 and 0.015, respectively, for a random sequence with the same shape at 37° C (figure 6.3C). There is computational evidence for such transposability in natural sequences (Wagner and Stadler, 1999).

While it is unclear how natural selection could generate modularity directly, there are many scenarios in which natural selection favors the reduction of plasticity. In our model, modularity arises as a necessary by-product of that reduction. It is the nature of modules to resist change; hence the process that produces modularity simultaneously leads populations into evolutionary dead ends. By enabling variation at a new syntactical level, however, modularity may provide an escape from the evolutionary trap that produced it in the first place.

In the future, we will study RNA structural evolution in a fluctuating environment. Evolutionary theory teaches us that phenotypic plasticity is favored under sufficiently heterogeneous conditions. When RNA molecules evolve under macroscopic fluctuations, for example, in the presence of multiple binding targets or changing temperatures, natural selection may produce plastic RNA molecules. We will evaluate this hypothesis, and ask whether fluctuating environments consequently favor evolvability and preclude the evolution of modularity.

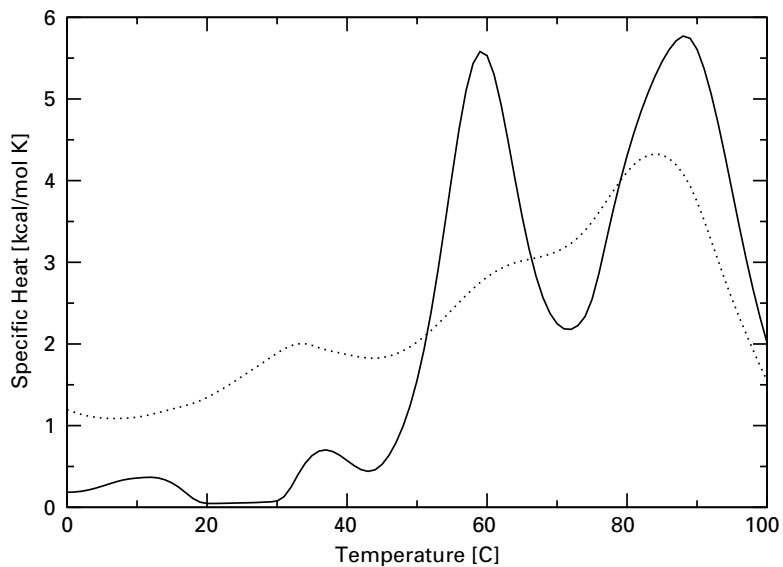
Acknowledgments

We thank Werner Callebaut and Diego Rasskin-Gutman for inviting our contributions to this volume and to the workshop on modularity at the Konrad Lorenz Institute. Thanks also to Ivo Hofacker, Peter Stadler, and Stefan Wuchty for their work on the Vienna RNA package. We are grateful to Leo Buss, Marc Feldman, Christoph

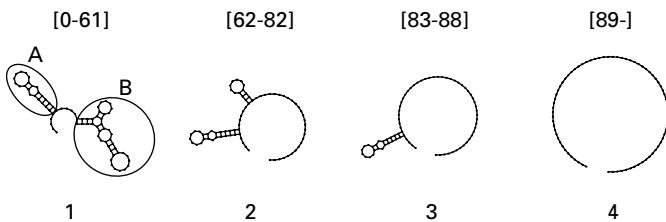
Figure 6.3

Thermophysical and kinetic modularity. (A) The calculated melting behavior (specific heat versus temperature) as it would appear in a differential scanning calorimetry experiment. The modular (evolved) RNA molecule (solid line) melts in two sharp phase transitions. The dotted line depicts the melting behavior of a high-plasticity sequence. (B) The ground states of the modular (evolved) RNA molecule as a function of temperature ($^{\circ}\text{C}$). The 37°C features have extended thermal stability, and melt individually at distinct temperatures while leaving other parts of the shape unaffected. In other words, the melting behavior is discrete. (C) The succession of ground states with rising temperature of a high-plasticity sequence with the same shape at 37°C as the evolved molecule in (B). The 37°C shape of the sequence is unstable upon temperature perturbations in both directions, and undergoes global rearrangements as the 37°C features destabilize with rising temperature. (D) Given a kinetic model of the folding process, the low-energy portion of a molecule's conformational landscape can be represented as a tree (Flamm et al., 2000). The ordinate measures free energy, and the abscissa has no meaning. A leaf corresponds to a shape at a local energy minimum, and the height of a branch point corresponds to the energy barrier between two local minima. (D) shows that the folding landscape of the evolved sequence is organized as a funnel leading directly to the ground state shape. Modules fold independently. (E) The energy landscape of the random sequence provides little or no guidance to the folding process, and results in frequent deadlocks at local minima.

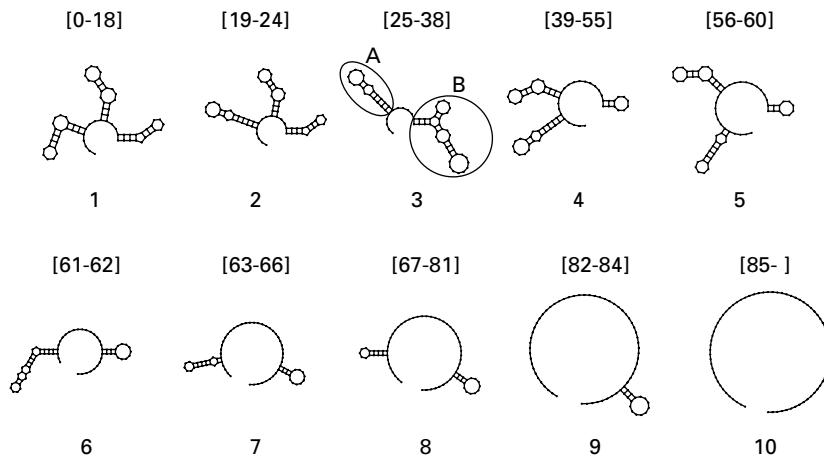
(a)



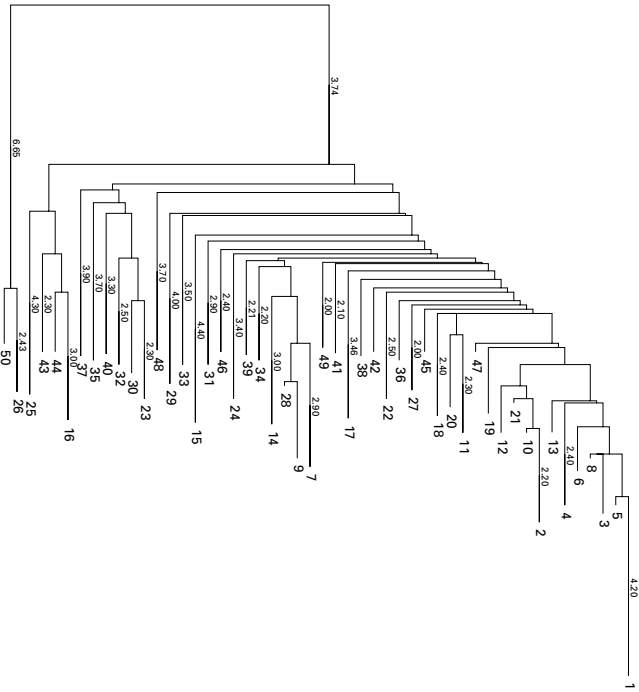
(b)



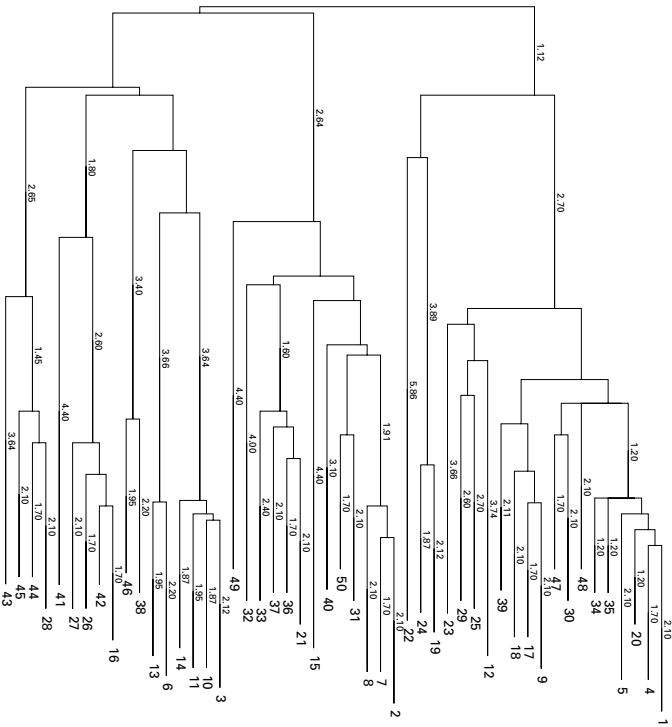
(c)



(d)



(e)



Flamm, Peter Godfrey-Smith, Ellen Goldberg, James Griesemer, Martijn Huynen, Erica Jen, Junhyong Kim, Michael Lachmann, Laura Landweber, Mark Newman, Erik van Nimwegen, Peter Schuster, Andreas Wagner, Günter Wagner, and Rasmus Winther for valuable discussions and comments on our manuscripts.

The research program of Walter Fontana at the Santa Fe Institute was supported by Michael A. Grantham. Partial support came from the Keck Foundation and an NSF grant to the Santa Fe Institute, an NIH grant to M. W. Feldman at Stanford, a U.S. National Defense Science and Engineering Fellowship to Lauren Ancel, a National Science Foundation Postdoctoral Fellowship to Lauren Ancel, and the Program in Theoretical Biology at the Institute for Advanced Study, Princeton, N.J.

References

- Ancel LW (1999) A quantitative model of the Simpson–Baldwin effect. *J Theor Biol* 196: 197–209.
- Ancel LW, Fontana W (2000) Plasticity, evolvability and modularity in RNA. *J Exp Zool (Mol Dev Evol)* 288: 242–283.
- Baldwin JM (1896) A new factor in evolution. *Amer Nat* 30: 441–451.
- Bonner JT (1988) *The Evolution of Complexity by Means of Natural Selection*. Princeton, NJ: Princeton University Press.
- Bornberg-Bauer E, Chan HS (1999) Modeling evolutionary landscapes: Mutational stability, topology, and superfunnels in sequence space. *Proc Natl Acad Sci USA* 96: 10689–10694.
- Bussemaker HJ, Thirumalai D, Bhattacharjee JK (1997) Thermodynamic stability of folded proteins against mutations. *Phys Rev Lett* 79: 3530–3533.
- Ellington AD (1994) RNA selection: Aptamers achieve the desired recognition. *Curr Biol* 4: 427–429.
- Flamm C, Fontana W, Hofacker IL, Schuster P (2000) RNA folding at elementary step resolution. *RNA* 6: 325–338.
- Fontana W, Schuster P (1998) Continuity in evolution: On the nature of transitions. *Science* 280: 1451–1455.
- Hartwell LH, Hopfield JJ, Leibler S, Murray AW (1999) From molecular to modular cell biology. *Nature* 402 supp.: C47–C52.
- Huynen MA, Stadler PF, Fontana W (1996) Smoothness within ruggedness: The role of neutrality in adaptation. *Proc Natl Acad Sci USA* 93: 397–401.
- McCaskill JS (1990) The equilibrium partition function and base pair binding probabilities for RNA secondary structure. *Biopolymers* 29: 1105–1119.
- Nussinov R, Jacobson AB (1980) Fast algorithm for predicting the secondary structure of single-stranded RNA. *Proc Natl Acad Sci USA* 77: 6309–6313.
- Simpson GG (1953) The Baldwin effect. *Evolution* 7: 110–117.
- Vendruscolo M, Maritan A, Banavar JR (1997) Stability threshold as a selection principle for protein design. *Phys Rev Lett* 78: 3967–3970.
- Wagner GP, Altenberg L (1996) Perspective: Complex adaptations and the evolution of evolvability. *Evolution* 50(3): 967–976.

Wagner A, Stadler PF (1999) Viral RNA and evolved mutational robustness. *J Exp Zool (Mol Dev Evol)* 285: 119–127.

Waterman MS (1978) *Secondary Structure of Single-stranded Nucleic Acids*. New York: Academic Press.

Westhof E, Masquida B, Jaeger L (1996) RNA tectonics: Towards RNA design. *Folding and Design* 1: R78–R88.

Wuchty S, Fontana W, Hofacker IL, Schuster P (1999) Complete suboptimal folding of RNA and the stability of secondary structures. *Biopolymers* 49: 145–165.

Zuker M, Stiegler P (1981) Optimal computer folding of larger RNA sequences using thermodynamics and auxiliary information. *Nucleic Acids Research* 9: 133–148.